Titre: Title:	The jacobian matrix for a flexible manipulator
Auteurs: Authors:	Jean-Claude Piedboeuf
Date:	1993
Type:	Rapport / Report
Référence: Citation:	Piedboeuf, J.-C. (1993). The jacobian matrix for a flexible manipulator. (Rapport technique n° EPM-RT-93-17). https://publications.polymtl.ca/10139/

EPM/RT-93/17

"THE JACOBIAN MATRIX FOR A FLEXIBLE MANIPULATOR"

par

Jean-Claude Piedboeuf

Département de Génie Electrique et Génie Informatique

Ecole Polytechnique de Montréal

1993

gratuit

Dépôt légal, septembre 1993
Bibliothèque nationale du Québec
Bibliothèque nationale du Canada

Pour se procurer une copie de ce document, s'adresser au:

Éditions de l'École Polytechnique de Montréal
École Polytechnique de Montréal
Case Postale 6079, Succursale A
Montréal (Québec) H3C 3A7
(514) 340-4000

Compter 0,10$ par page (arrondir au dollar le plus près) et ajouter 3,00$ (Canada) pour la couverture, les frais de poste et la manutention. Régler en dollars canadiens par chèque ou mandat-poste au nom de l'École Polytechnique de Montréal. Nous n'honorerons que les commandes accompagnées d'un paiement, sauf s'il y a eu entente préalable dans le cas d'établissements d'enseignement, de sociétés ou d'organismes canadiens.

The Jacobian Matrix for a Flexible Manipulator

Jean-Claude Piedbœuf*

July 30, 1993

Abstract

This paper develops the exact first order endpoint Jacobian matrix for a general n degrees of freedom tree-like robot with flexible links. The Jacobian is developed in terms of the joint axis, the link deformations and the relative position vectors using cross products. To have the correct first order endpoint Jacobian matrix, the second order kinematics is used to describe a flexible link. Using two local Jacobian matrices permits one to write the endpoint Jacobian sub-matrix associated to a flexible link which is similar to the column of the Jacobian associated to a joint. An example with a one link flexible arm rotating in a vertical plane illustrates the usefulness of the endpoint Jacobian in calculating the torque required to apply an endpoint force and the link deformation resulting from this force. An experimental verification proves the validity of the developed Jacobian and suggests that the use of only the first order kinematics, results in serious errors in the prediction of the beam's curvatures and deformations.

1 Introduction

In robotics the Jacobian matrix relates the motions or the forces of the cartesian space to the robot space. For example, for a rigid robot, the Jacobian matrix gives the end-effector velocities for a given set of joint velocities, or permits computation of the joint forces and torques required to obtain a desired force and torque at the end-effector. The Jacobian is implemented in some controllers like the resolved rate or the force control (Orin and Schrader 1984). For flexible robots, the Jacobian matrix is used to write the equations of motion using Jourdain's principle (Bremer 1987, Pfeiffer and Bremer 1990, Lieh 1992) and Lagrange's form of d'Alembert's principle (Weng and Greenwood 1992), or to add the constraints to the dynamic equations (Ider and Amirouche 1989, Pfeiffer et al. 1990). When controlling flexible robots, the Jacobian matrix is employed to compute the inverse kinematics (Williams and Turcic 1992), to analyze the dynamic stability of a force controlled flexible manipulator (Chiou and Shahinpoor 1990) and to obtain a torque/force relationship and kinematics representation (Kozel et al. 1991).

In the case of rigid manipulators, different possibilities exist for computing the Jacobian matrix and these have been the focus of many published papers (see Orin and Schrader 1984 for a discussion about the efficiency of some of these approaches). The first and simplest

*Assistant Professor, Mechanical Engineering Department, Royal Military College of Canada, Kingston, Ontario, Canada, K7K 5L0, also Adjunct Professor, Electrical Engineering Department, École Polytechnique de Montréal

way to compute the Jacobian is to take the partial derivatives of the velocities with respect to the generalized velocities. A second and more computer-oriented way is to calculate the Jacobian recursively starting from the base. This method requires the computation of n Jacobians for a n degrees of freedom manipulator and is not practical when only the endpoint Jacobian is needed. However it is very efficient if the intermediate Jacobians are required as in Jourdain's principle. A third approach consists of writing the coefficients of the endpoint Jacobian matrix in terms of the joint axis and relative position vectors using cross products. This last approach is the foundation of many efficient methods to compute the endpoint Jacobian.

Relative to a rigid manipulator a flexible manipulator possesses additional degrees of freedom. However, while rigid motion is considered to be arbitrarily large, the motion resulting from the flexibility is assumed to be small. This small deformation assumption is common in nearly all research work concerning flexible manipulators. This assumption implies that the terms of second order or higher, involving generalized coordinates associated with the flexibility, are negligible in the equations of motion. These equations are then exact to the first order. It is now recognized that the equations of motion exact to the first order must include the so-called *geometric stiffening terms* (Hodges et al. 1980, Simo and Vu Quoc 1987, Padilla and von Flotow 1992, Sharf 1993). It is also accepted that these stiffening terms are related to the foreshortening of the flexible link (Kaza and Kvaternik 1977) and are introduced into the equations through the nonlinear strain-displacement relationships. The foreshortening is the fact that a beam element at position x along the neutral axis in the undeformed state is no longer at position x in the deformed state. However, it is not widely recognized that for the Jacobian matrix of a flexible manipulator to be exact to the first order, the kinematics must be developed up to the second order. Also, the geometric stiffening is often regarded as being caused by the angular speed (Padilla and von Flotow 1992). They are however, essential for considering high angular velocities, high accelerations and large endpoint forces. As shown in this paper, neglecting these terms, even for a static case, results in serious errors.

Some research has already been done on the Jacobian matrix for flexible manipulators. Probably the oldest and most complete work originates from the Technical University of Munich (Bremer 1983, Bremer 1985, Johanni 1985, Johanni 1986, Pfeiffer and Bremer 1990, Bremer and Pfeiffer 1992) . A first order Jacobian matrix was developed for a general manipulator with flexible links using second order kinematics with the curvatures and the twist as generalized coordinates. The Jacobian is calculated recursively starting from the base as in the aforementioned second approach. In another work, Chiou and Shahinpoor (1990) developed the endpoint Jacobian for a two-link flexible manipulator moving in the horizontal plane considering only the small deformations within the plane. They kept the rotation angle of a beam section as an argument of the sine and the cosine without taking a first order expansion as usual with the small deformation assumption (e.g. $\sin\theta \approx \theta$). Still they did not consider the foreshortening of the beam, therefore their Jacobian is not exact to the first order. Chang and Hamilton (1991) developed a *generalized Jacobian*, a Jacobian matrix which includes the effects of the flexible links for a general robot. They considered one longitudinal and two bending deformations as well as the torsion around the longitudinal axis. However, they did not include the rotations of a beam section due to the bending displacements. For a Euler-Bernoulli beam, these rotations are equal to the first derivative of the deformations with respect to x, the variable along the longitudinal axis. Furthermore, they did not consider the foreshortening. Therefore, their Jacobian is incorrect. By applying the third approach discussed for a rigid robot, Kozel et al. (1991) developed a general endpoint *pseudo Jacobian* for any flexible manipulator. They used homogeneous transformations and Euler-Bernoulli beam theory. They assumed two bending deformations and one torsion plus the two rotations due to the bending, adding up to five possible motions. In their approach, a column of the endpoint Jacobian is computed independently for each of the five possible motions. They pointed out that the Jacobian obtained through partial derivatives of the velocities is inexact since $\cos\phi(x) = 1$ with a small angle assumption and $\partial \cos\phi(x)/\partial x \neq \partial(1)/\partial x$. Still, they did not state that all the kinematics must be exact to the second order and their Jacobian is not correct to the first order. However, through an experimental validation they show that they can predict the joint torque for a one link flexible arm. As shown in this paper, using only first order kinematics does not affect significantly the joint torque but affects the endpoint position and curvature values.

The main contribution of this paper is the development of an endpoint Jacobian matrix exact to the first order for a general flexible manipulator. The second order kinematics is based on the use of the curvatures and the twist as generalized coordinates (Johanni 1986). We will write the Jacobian in terms of the joint axis, the link deformations and the relative position vectors using cross products. Contrarily to Kozel et al. (1991) , all the columns of the endpoint Jacobian matrix related to a flexible link are calculated in one step. In Section 2, we discuss the different assumptions, we establish a general form for the Jacobian matrix and we introduce the Jacobian column associated with a joint. Further, we present thoroughly the kinematics of a flexible beam, write two local Jacobian matrices and obtain the Jacobian sub-matrix corresponding to a flexible link. In Section 3, we develop an example using a one-link flexible arm rotating in a vertical plane. Finally, in Section 4, we compare the experimental and the simulation results and discuss the contributions of the terms originating from the second order kinematics.

2 The Jacobian

2.1 General Formulation of the Jacobian

This section develops the general form of the Jacobian for a n degrees of freedom flexible robot. First, the generalized coordinates are described and the contributions of the joints and those of the flexible bodies are considered. Later, the different frames used are presented and the Jacobian for a rigid body is briefly discussed. The main emphasis of this section concerns the analytical development of the Jacobian for a flexible link.

Let us consider a robot with n_r joints and n_{fb} flexible links. The following assumptions are made in this paper:

A1) The links are considered as Euler-Bernoulli beams, implying that:

a) beam section's shear effect and inertia of rotation are ignored;

b) beam sections stay plane and perpendicular to the neutral axis.

A2) One torsional and two bending deformations are considered. The warping of the beam is neglected.

A3) The neutral axis is non-extensible. Hence, the longitudinal deformation is ignored.

A4) The assumed mode method is used to discretize a flexible link. Therefore, n_{f_i} generalized coordinates are associated with the flexible link i. The total number of generalized coordinates associated with the flexible links is: $n_f = \sum_{i=1}^{n_{fb}} n_{f_i}$.

A5) The deformations are small (max deflection < 10 % of the length, or 15^o max for the rotation) and only first order terms related to the coordinates associated with the flexibility are retained in the final equations of motion.

A6) Joint motions are arbitrarily large and consequently, the coordinates associated with rigid body motion are considered to be large (or zero order).

A7) The system is completely described by the vector of generalized coordinates: $\boldsymbol{q} = [\boldsymbol{q}_r^T, \boldsymbol{q}_f^T]^T$ where the dimension of $\boldsymbol{q}$ is $n = n_r + n_f$.

The following notation is used throughout this paper: a normal italic font for a scalar - s, a boldface italic for a vector - $\boldsymbol{v}$, and an upper-case boldface italic for a matrix - $\boldsymbol{M}$. We denote the partial derivative with respect to time by $\dot{()}$ and the partial derivative with respect to space by $()'$. The generalized coordinates associated with the rigid body motion are called rigid coordinates while the ones associated with the flexible links are called flexible coordinates. Unless otherwise specified, the vectors and matrices are expressed in the inertial reference frame.

The endpoint Jacobian relates the endpoint velocity to the generalized velocities:

$$\begin{bmatrix} \boldsymbol{v}_e \\ \boldsymbol{\omega}_e \end{bmatrix} = \boldsymbol{J}_e \dot{\boldsymbol{q}} = \begin{bmatrix} \boldsymbol{J}_{T,e} \\ \boldsymbol{J}_{R,e} \end{bmatrix} \dot{\boldsymbol{q}} \tag{1}$$

where $\boldsymbol{J}_{T,e}$ and $\boldsymbol{J}_{R,e}$ are respectively the endpoint Jacobians of translation and of rotation. The Jacobian reflects the influence of the infinitesimal displacement of the generalized coordinates on the endpoint infinitesimal motion.

The endpoint Jacobian is separated according to the generalized coordinates' division into rigid and flexible coordinates.

$$\boldsymbol{J}_e = \underbrace{\begin{bmatrix} (\boldsymbol{J}_{T,e})_{j_1} & \cdots & (\boldsymbol{J}_{T,e})_{j_{n_r}}, \\ (\boldsymbol{J}_{R,e})_{j_1} & \cdots & (\boldsymbol{J}_{R,e})_{j_{n_r}}, \end{bmatrix.}_{joints} \underbrace{\begin{matrix} (\boldsymbol{J}_{T,e})_{f_1} & \cdots & (\boldsymbol{J}_{T,e})_{f_{n_{fb}}} \\ (\boldsymbol{J}_{R,e})_{f_1} & \cdots & (\boldsymbol{J}_{R,e})_{f_{n_{fb}}} \end{matrix} \Bigg]}_{flexible\ bodies} \tag{2}$$

$$(\boldsymbol{J}_{T,e})_{j_i}, (\boldsymbol{J}_{R,e})_{j_i}, \in \Re^3, \quad (\boldsymbol{J}_{T,e})_{f_i}, (\boldsymbol{J}_{R,e})_{f_i} \in \Re^{3,n_{f_i}}$$

where $\boldsymbol{J}_T$ and $\boldsymbol{J}_R$ represent the Jacobian matrices of translation and of rotation. There are n_r columns for the n_r joints and n_{fb} sub-matrices for the n_{fb} flexible links. The sub-matrix associated to the flexible body i comprises n_{f_i} columns, which is the number of degrees of freedom associated to the flexible link i.

Figure 1 shows a general robot with its frames, and Figure 2 gives the details of a flexible link i. Joint i has an associated frame $\mathcal{R}_i$ (Fig. 1), and flexible body i has frame $\mathcal{R}_i$ attached to its extremity (Fig. 2).

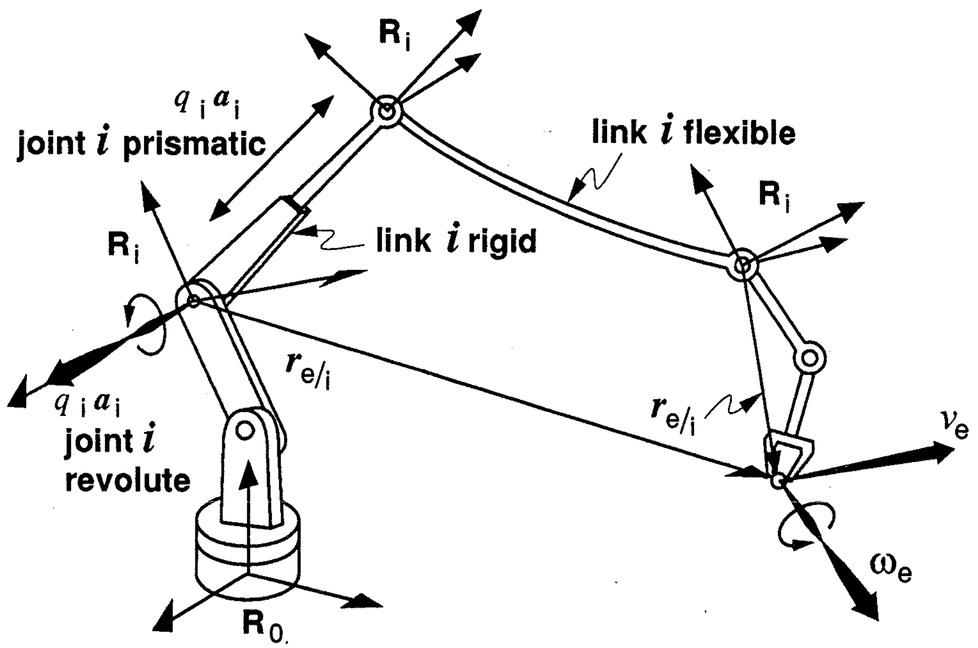

Figure 1: A general n degree of freedom robot

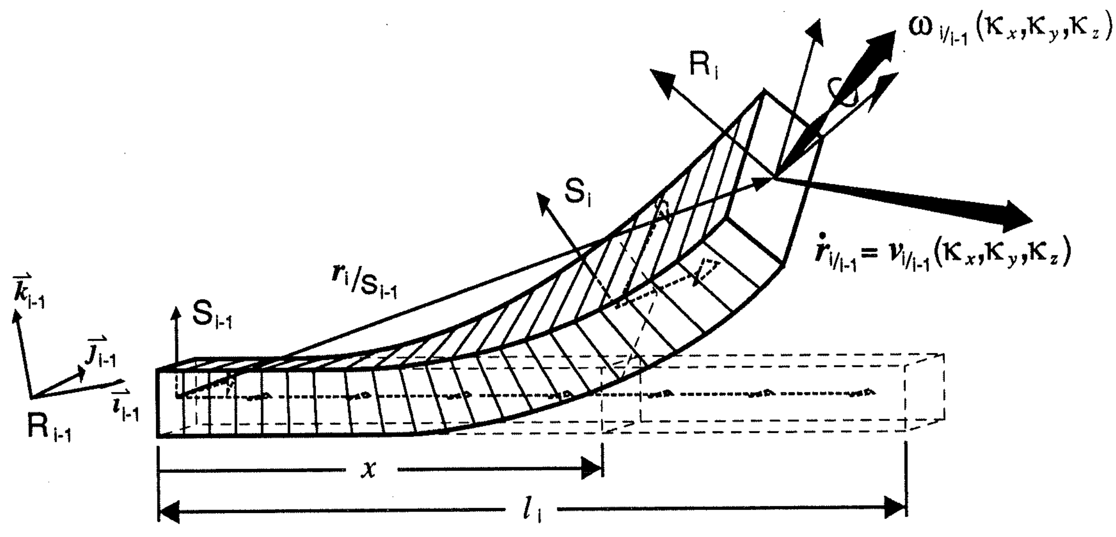

Figure 2: The flexible link i and its frames

2.2 Joints

The endpoint Jacobian for a joint is the same as the one for a rigid robot and is developed in many robotic textbooks (Orin and Schrader 1984, Asada and Slotine 1986. The following equation expresses the endpoint Jacobian directly in terms of the robot parameters:

$$(\boldsymbol{J}_e)_{j_i} = \begin{bmatrix} (\boldsymbol{J}_{T,e})_{j_i} \\ (\boldsymbol{J}_{R,e})_{j_i} \end{bmatrix} = \begin{bmatrix} \boldsymbol{a}_i \times \boldsymbol{r}_{e/i}\sigma_i + \boldsymbol{a}_i(1-\sigma_i) \\ \boldsymbol{a}_i\sigma_i \end{bmatrix} \in \Re^6 \tag{3}$$

$$\sigma_i = \begin{cases} 1 & \text{if joint } i \text{ is revolute} \\ 0 & \text{if joint } i \text{ is prismatic} \end{cases}$$

In (3), $\boldsymbol{r}_{e/i}$ is the position of the robot endpoint with respect to the origin of frame $\mathcal{R}_i$ located at joint i (Fig. 1), and $\boldsymbol{a}_i$ is the motion axis of joint i. Since $\boldsymbol{a}_i$ is constant in the frame $\mathcal{R}_i$, we use the following transformation:

$$\boldsymbol{a}_i = \boldsymbol{R}_i^0 \, {}^i\boldsymbol{a}_i \tag{4}$$

where $\boldsymbol{R}_i^0$ represents the rotation matrix from the moving frame $\mathcal{R}_i$ to the inertial frame $\mathcal{R}_0$. The superscript i in ${}^i\boldsymbol{a}_i$ denotes that $\boldsymbol{a}_i$ is expressed in $\mathcal{R}_i$. Equation (3) signifies that for a prismatic joint, the endpoint displacement is only in translation and directly corresponds to joint motion. On the other hand, a revolute joint generates both an angular displacement of the endpoint frame equal to the joint rotation and a linear displacement.

2.3 Flexible Body

When a flexible link deforms, its motion affects all the bodies situated after that link and therefore the robot endpoint. The endpoint Jacobian sub-matrix $(\boldsymbol{J}_e)_{f_i}$ (2) represents the influence of the movement of the flexible link i extremity on the robot endpoint. Flexible-body motion is more complex than joint motion since a link's extremity has both a translation movement $\dot{\boldsymbol{r}}_{i/i-1}$ and a rotation movement $\boldsymbol{\omega}_{i/i-1}$ with respect to its root (Fig. 2). The translation can be associated to a prismatic joint, and the rotation to a revolute joint. In contrast to a joint, motions are not restricted to one axis and occur simultaneously. The endpoint velocities $(\boldsymbol{v}_e)_{f_i}$ and $(\boldsymbol{\omega}_e)_{f_i}$ (Fig. 1) due to the flexible body i motion are defined as follows:

$$(\boldsymbol{v}_e)_{f_i} = (\boldsymbol{J}_{T,e})_{f_i}\dot{\boldsymbol{q}}_{f_i} = \dot{\boldsymbol{r}}_{i/i-1} + \boldsymbol{\omega}_{i/i-1} \times \boldsymbol{r}_{e/i} \tag{5}$$

$$(\boldsymbol{\omega}_e)_{f_i} = (\boldsymbol{J}_{R,e})_{f_i}\dot{\boldsymbol{q}}_{f_i} = \boldsymbol{\omega}_{i/i-1} \tag{6}$$

where $\boldsymbol{r}_{e/i}$ is the position vector of the robot endpoint with respect to flexible link i endpoint (Fig. 1). The middle terms of (5) simply apply the definition of the Jacobian while the right hand terms express the endpoint velocity due to flexible link i motion as a function of velocity $\dot{\boldsymbol{r}}_{i/i-1}$ and angular speed $\boldsymbol{\omega}_{i/i-1}$.

2.3.1 Linear and angular velocities for a flexible link

Reference frames To obtain $\dot{\boldsymbol{r}}_{i/i-1}$ and $\boldsymbol{\omega}_{i/i-1}$, we use three different reference frames for flexible link i (Fig. 2):

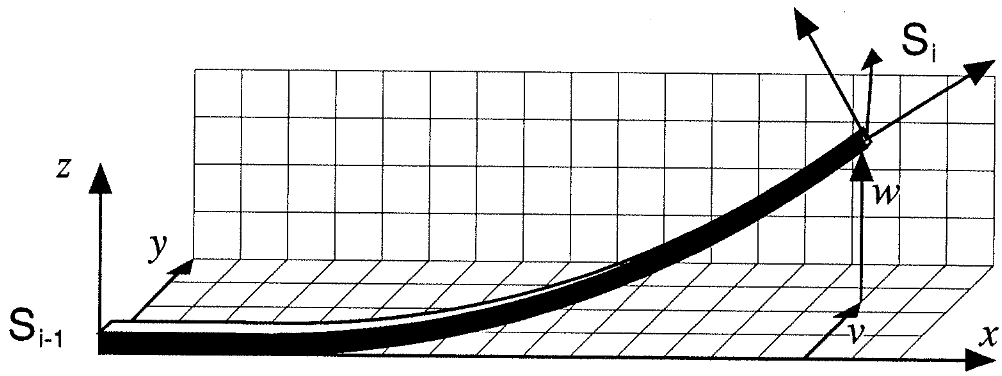

Figure 3: A flexible arm with v and w as coordinates

1) A frame $\mathcal{S}_{i-1}$ is attached to the link root. The x-axis of this frame is tangent to the link neutral axis. A constant transformation couples this frame to the frame $\mathcal{R}_{i-1}$ attached to joint $i-1$. To simplify the presentation, without loss of generality[1], we assume that frames $\mathcal{S}_{i-1}$ and $\mathcal{R}_{i-1}$ are superimposed at the link root (at $x=0$).

2) A frame $\mathcal{S}_i$ is attached to a beam section at position x along the link. This frame is superimposed on $\mathcal{S}_{i-1}$ at the link root. Assumption A1b is equivalent to stating that the x-axis of $\mathcal{S}_i$ is tangent to the neutral axis.

3) A frame $\mathcal{R}_i$ is attached to the link extremity. This frame coincides with frame $\mathcal{S}_i$ when $x = l_i$.

Finding $\dot{\boldsymbol{r}}_{i/i-1}$ and $\boldsymbol{\omega}_{i/i-1}$ is now equivalent to developing the transformation between $\mathcal{R}_i$ and $\mathcal{R}_{i-1}$. As a step towards that goal, we first obtain the rotation matrix and the position vector between $\mathcal{S}_i$ and $\mathcal{S}_{i-1}$.

Rotation matrix We need a set of coordinates to determine the relationship between the two frames $\mathcal{S}_i$ and $\mathcal{S}_{i-1}$. Since second order terms are retained in the kinematics, the choice of coordinates to represent the rotations becomes more delicate (Hodges et al. 1980). By using a set of angles, such as Euler angles, the resulting rotation matrix will vary depending upon the order in which these angles are considered.

For example, Figure 3 shows a flexible arm with the widely used coordinates v and w. Using assumption A1, we define v' as a rotation around z and $-w'$ as a rotation around y. Considering first a rotation v' followed by a rotation $-w'$, and developing to the first and to the second order, results in the following expression for the rotation matrix $\boldsymbol{R}_{\mathcal{S}_i}^{\mathcal{S}_{i-1}}$ from $\mathcal{S}_i$ to $\mathcal{S}_{i-1}$:

$$(\boldsymbol{R}_{\mathcal{S}_i}^{\mathcal{S}_{i-1}})^{v'w'} \overset{\mathcal{O}(1)}{=} \begin{bmatrix} 1 & -v' & -w' \\ v' & 1 & 0 \\ w' & 0 & 1 \end{bmatrix} \overset{\mathcal{O}(2)}{=} \begin{bmatrix} 1-\frac{1}{2}(v'^2+w'^2) & -v' & -w' \\ v' & 1-\frac{1}{2}v'^2 & -v'w' \\ w' & 0 & 1-\frac{1}{2}w'^2 \end{bmatrix} \tag{7}$$

[1]Since we work with velocity, a constant transformation does not make a difference.

Now reversing the order of rotation, $-w'$ before v', produces the following rotation matrices to the first and second order:

$$(\boldsymbol{R}_{\mathcal{S}_i}^{\mathcal{S}_{i-1}})^{w'v'} \stackrel{\mathcal{O}(1)}{=} \begin{bmatrix} 1 & -v' & -w' \\ v' & 1 & 0 \\ w' & 0 & 1 \end{bmatrix} \stackrel{\mathcal{O}(2)}{=} \begin{bmatrix} 1-\frac{1}{2}(v'^2+w'^2) & -v' & -w' \\ v' & 1-\frac{1}{2}v'^2 & 0 \\ w' & -v'w' & 1-\frac{1}{2}w'^2 \end{bmatrix} \tag{8}$$

There is no difference between (7) and (8) for the first order rotation matrix ($\mathcal{O}(1)$) however the second order matrices ($\mathcal{O}(2)$) are different (permutation of the elements (2,3) and (3,2)). This result is disturbing since, for a flexible link, the rotations around the different axes take place simultaneously, independently of the order of the kinematics.

In order to avoid this discrepancy, we use the rate of twist κ_x and the local bending curvatures κ_y and κ_z as coordinates. This approach has been proposed by Johanni (1985) and is described in Bremer and Pfeiffer (1992) . The vector $\boldsymbol{\kappa}$ represents the derivative of the angles with respect to the space variable x as defined by the following equation:

$$\boldsymbol{\kappa} = \lim_{\Delta x \to 0} \frac{\Delta \boldsymbol{\theta}}{\Delta x} \tag{9}$$

The same kind of relation exists between the rotation matrix $\boldsymbol{R}_{\mathcal{S}_i}^{\mathcal{S}_{i-1}}$ (from $\mathcal{S}_i$ to $\mathcal{S}_{i-1}$) and $\boldsymbol{\kappa}$ as between the rotation matrix and the angular velocity vector $\boldsymbol{\omega}$. As demonstrated in Appendix A, this relation leads to the following differential equation:

$$^{\mathcal{S}_i}\tilde{\boldsymbol{\kappa}} = \begin{bmatrix} 0 & -\kappa_z & \kappa_y \\ \kappa_z & 0 & -\kappa_x \\ -\kappa_y & \kappa_x & 0 \end{bmatrix} = \boldsymbol{R}_{\mathcal{S}_{i-1}}^{\mathcal{S}_i} \frac{d\boldsymbol{R}_{\mathcal{S}_i}^{\mathcal{S}_{i-1}}}{dx} \quad \Longrightarrow \quad \frac{d\boldsymbol{R}_{\mathcal{S}_i}^{\mathcal{S}_{i-1}}}{dx} = \boldsymbol{R}_{\mathcal{S}_i}^{\mathcal{S}_{i-1}}\,{}^{\mathcal{S}_i}\tilde{\boldsymbol{\kappa}} \tag{10}$$

where x is the distance along the neutral axis (Fig. 2). Superscript $\mathcal{S}_i$ in $^{\mathcal{S}_i}\tilde{\boldsymbol{\kappa}}$ denotes that $\boldsymbol{\kappa}$ is defined in frame $\mathcal{S}_i$, and the tilde symbol $\tilde{}$ indicates that $\tilde{\boldsymbol{\kappa}}$ is the skew-symmetric matrix formed with the elements of $\boldsymbol{\kappa}$.

The rotation matrix can now be found by solving the differential equation (10). This is achieved by first developping the rotation matrix $\boldsymbol{R}_{\mathcal{S}_i}^{\mathcal{S}_{i-1}}$ up to the second order:

$$\boldsymbol{R}_{\mathcal{S}_i}^{\mathcal{S}_{i-1}} = \boldsymbol{R}_0 + \boldsymbol{R}_1 + \boldsymbol{R}_2 \tag{11}$$

where $\boldsymbol{R}_0$ is the identity matrix. Then, using assumption A5, we conclude that $^{\mathcal{S}_i}\tilde{\boldsymbol{\kappa}}$, being the flexible coordinates, comprises only first order terms. We replace (10) by the following differential equation:

$$\underbrace{\frac{d\boldsymbol{R}_1}{dx}}_{\mathcal{O}(1)} + \underbrace{\frac{d\boldsymbol{R}_2}{dx}}_{\mathcal{O}(2)} = \underbrace{^{\mathcal{S}_i}\tilde{\boldsymbol{\kappa}}}_{\mathcal{O}(1)} + \underbrace{\boldsymbol{R}_1{}^{\mathcal{S}_i}\tilde{\boldsymbol{\kappa}}}_{\mathcal{O}(2)} + \underbrace{\boldsymbol{R}_2{}^{\mathcal{S}_i}\tilde{\boldsymbol{\kappa}}}_{\mathcal{O}(3)} \tag{12}$$

Let us integrate separately the same order terms of (12) to obtain the following expressions for $\boldsymbol{R}_1$ and $\boldsymbol{R}_2$:

$$\boldsymbol{R}_1 = \int_0^x {}^{\mathcal{S}_i}\tilde{\boldsymbol{\kappa}}\, d\xi \tag{13}$$

$$\boldsymbol{R}_2 = \int_0^x \boldsymbol{R}_1{}^{\mathcal{S}_i}\tilde{\boldsymbol{\kappa}}\, d\xi \tag{14}$$

since $\boldsymbol{R}_1(0)$ and $\boldsymbol{R}_2(0)$ are null matrices ($\mathcal{S}_i$ corresponds to $\mathcal{S}_{i-1}$ for $x = 0$). The solutions of (13) and (14) in terms of $\boldsymbol{\kappa}$ are in Appendix B. We will now use the following definitions to simplify the notation:

$$v = \int_0^x \int_0^\xi \kappa_z d\eta d\xi \quad w = -\int_0^x \int_0^\xi \kappa_y d\eta d\xi \quad \alpha = \int_0^x \kappa_x d\xi \tag{15}$$

where v and w represent pure bending deflections while α represents a pure torsion angle. Explicit calculation of the right hand side of (13) and (14) in conjunction with (11) and (15) gives the following expression for the rotation matrix $\boldsymbol{R}_{\mathcal{S}_i}^{\mathcal{S}_{i-1}}$:

$$\boldsymbol{R}_{\mathcal{S}_i}^{\mathcal{S}_{i-1}} = \begin{bmatrix} 1 - \frac{1}{2}(v'^2 + w'^2) & -v' - \int_0^x \alpha' w'\, d\xi & -w' + \int_0^x \alpha' v'\, d\xi \\ v' - \int_0^x \alpha w''\, d\xi & 1 - \frac{1}{2}(v'^2 + \alpha^2) & -\alpha - \int_0^x v' w''\, d\xi \\ w' + \int_0^x \alpha v''\, d\xi & \alpha - \int_0^x v'' w'\, d\xi & 1 - \frac{1}{2}(w'^2 + \alpha^2) \end{bmatrix} \tag{16}$$

Position vector To obtain the position vector $\boldsymbol{r}_{\mathcal{S}_{i-1},\mathcal{S}_i}$ from the origin of frame $\mathcal{S}_{i-1}$ to the origin of frame $\mathcal{S}_i$, we use the assumptions A1b and A3. These assumptions are mathematically formalized as follows:

$$\frac{{}^{\mathcal{S}_{i-1}}\boldsymbol{r}'_{\mathcal{S}_{i-1},\mathcal{S}_i}}{|\boldsymbol{r}'|} = \boldsymbol{R}_{\mathcal{S}_i}^{\mathcal{S}_{i-1}} \begin{bmatrix} 1 \\ 0 \\ 0 \end{bmatrix} \text{ and } |\boldsymbol{r}'| = 1 \tag{17}$$

Using $\boldsymbol{r}(0) = 0$ and the rotation matrix (16), allows us to solve ordinary differential equation (17) for $\boldsymbol{r}_{\mathcal{S}_{i-1},\mathcal{S}_i}$ to obtain (Appendix B contains the solution in terms of $\boldsymbol{\kappa}$):

$${}^{\mathcal{S}_{i-1}}\boldsymbol{r}_{\mathcal{S}_{i-1},\mathcal{S}_i} = \int_0^x \boldsymbol{R}_{\mathcal{S}_i}^{\mathcal{S}_{i-1}} \begin{bmatrix} 1 \\ 0 \\ 0 \end{bmatrix} d\xi = \begin{bmatrix} x - \frac{1}{2}\int_0^x (v'^2 + w'^2)\, d\xi \\ v - \int_0^x \int_0^\xi w'' \alpha\, d\eta\, d\xi \\ w + \int_0^x \int_0^\xi v'' \alpha\, d\eta\, d\xi \end{bmatrix} \tag{18}$$

Velocities From the rotation matrix and the position vector, it is possible to determine the angular and the linear velocities of the frame attached to the link extremity with respect to the frame attached to the joint on which the link is fixed. The angular velocity $\boldsymbol{\omega}_{i/i-1}$ of frame $\mathcal{R}_i$ with respect to frame $\mathcal{R}_{i-1}$ is expressed in terms of rotation matrix $\boldsymbol{R}_i^{i-1}$ (which is obtained from $\boldsymbol{R}_{\mathcal{S}_i}^{\mathcal{S}_{i-1}}$ (16) with $x = l_i$)[2] using the following equation:

$${}^{i-1}\tilde{\boldsymbol{\omega}}_{i/i-1} = \begin{bmatrix} 0 & -\omega_z & \omega_y \\ \omega_z & 0 & -\omega_x \\ -\omega_y & \omega_x & 0 \end{bmatrix} = \frac{d\boldsymbol{R}_i^{i-1}}{dt}(\boldsymbol{R}_i^{i-1})^T \tag{19}$$

[2]If $\mathcal{S}_{i-1}$ and $\mathcal{R}_{i-1}$ do not have the same orientation, a constant rotation matrix is added: $R_i^{i-1} = R_{\mathcal{S}_{i-1}}^{i-1} R_{\mathcal{S}_i}^{\mathcal{S}_{i-1}}(x = l_i)$.

where the tilde $\tilde{}$ has the same signification as previously mentionned. Neglecting terms of order higher than two in (19) and rearranging to show the skew-symmetricalness, we obtain:

$$ {}^{i-1}\boldsymbol{\omega}_{i/i-1} = \begin{bmatrix} \dot{\alpha}_{l_i} + \displaystyle\int_0^{l_i} (v'\dot{w}'' - w'\dot{v}'')dx \\ -\dot{w}'_{l_i} - \displaystyle\int_0^{l_i} (\alpha\dot{v}'' - v'\dot{\alpha}')dx \\ \dot{v}'_{l_i} + \displaystyle\int_0^{l_i} (w'\dot{\alpha}' - \alpha\dot{w}'')dx \end{bmatrix} \tag{20} $$

The linear velocity $\dot{\boldsymbol{r}}_{i/i-1}$ is calculated by differentiating (18) with respect to time (using $x = l_i$) and gives the following result:

$$ {}^{i-1}\dot{\boldsymbol{r}}_{i/i-1} = \begin{bmatrix} -\displaystyle\int_0^{l_i} (v'\dot{v}' + w'\dot{w}')dx \\ \dot{v}_{l_i} - \displaystyle\int_0^{l_i}\int_0^{x} \dot{w}''\alpha + w''\dot{\alpha}d\xi dx \\ \dot{w}_{l_i} + \displaystyle\int_0^{l_i}\int_0^{x} \dot{v}''\alpha + v''\dot{\alpha}d\xi dx \end{bmatrix} \tag{21} $$

Discretization The deflections v and w, as well as the torsion α, depend on the space x and on the time t. To express v, w and α in terms of $\boldsymbol{q}_{f_i}$, the set of discrete coordinates for the flexible link i, we use the assumed mode method (Meirovitch 1967) as follows:

$$ \begin{bmatrix} v_i(x_i,t) \\ w_i(x_i,t) \\ \alpha_i(x_i,t) \end{bmatrix} = \boldsymbol{\Phi}_i(x_i)\boldsymbol{q}_{f_i} = \begin{bmatrix} {}^v\boldsymbol{\phi}_i^T(x_i) & 0 & 0 \\ 0 & {}^w\boldsymbol{\phi}_i^T(x_i) & 0 \\ 0 & 0 & {}^\alpha\boldsymbol{\phi}_i^T(x_i) \end{bmatrix} \begin{bmatrix} {}^v\boldsymbol{\eta}_i(t) \\ {}^w\boldsymbol{\eta}_i(t) \\ {}^\alpha\boldsymbol{\eta}_i(t) \end{bmatrix} \tag{22} $$

$$ {}^v\boldsymbol{\phi}_i, {}^v\boldsymbol{\eta}_i \in \Re^{\nu_{v_i}} \ , \ {}^w\boldsymbol{\phi}_i, {}^w\boldsymbol{\eta}_i \in \Re^{\nu_{w_i}} \ , \ {}^\alpha\boldsymbol{\phi}_i, {}^\alpha\boldsymbol{\eta}_i \in \Re^{\nu_{\alpha_i}} \ , \ q_{f_i} \in \Re^{n_{f_i}} $$

with $n_{f_i} = \nu_{v_i} + \nu_{w_i} + \nu_{\alpha_i}$

Local Jacobian matrices It is now possible to find two local Jacobian matrices which relate the link extremity to its root. The local Jacobian matrix of rotation is calculated from (20) as follows:

$$ {}^{i-1}\boldsymbol{J}_{R,i/i-1} = \frac{\partial^{i-1}\boldsymbol{\omega}_{i/i-1}}{\partial\dot{\boldsymbol{q}}_{f_i}} = \tag{23} $$

$$ \begin{bmatrix} -{}^w\boldsymbol{\eta}_i^T \int_0^{l_i} {}^w\boldsymbol{\phi}_i'{}^v\boldsymbol{\phi}_i''^T dx & {}^v\boldsymbol{\eta}_i^T \int_0^{l_i} {}^v\boldsymbol{\phi}_i'{}^w\boldsymbol{\phi}_i''^T dx & {}^\alpha\boldsymbol{\phi}_{l_i}^T \\ -{}^\alpha\boldsymbol{\eta}_i^T \int_0^{l_i} {}^\alpha\boldsymbol{\phi}_i'{}^v\boldsymbol{\phi}_i''^T dx & -{}^w\boldsymbol{\phi}_{l_i}'^T & {}^v\boldsymbol{\eta}_i^T \int_0^{l_i} {}^v\boldsymbol{\phi}_i'{}^\alpha\boldsymbol{\phi}_i'^T dx \\ {}^v\boldsymbol{\phi}_{l_i}'^T & -{}^\alpha\boldsymbol{\eta}_i^T \int_0^{l_i} {}^\alpha\boldsymbol{\phi}_i'{}^w\boldsymbol{\phi}_i'^T dx & {}^w\boldsymbol{\eta}_i^T \int_0^{l_i} {}^w\boldsymbol{\phi}_i'{}^\alpha\boldsymbol{\phi}_i'^T dx \end{bmatrix} $$

And the local Jacobian matrix of translation is calculated from (21) to give the following expression:

$$ {}^{i-1}\boldsymbol{J}_{T,i/i-1} = \frac{\partial^{i-1}\dot{\boldsymbol{r}}_{i/i-1}}{\partial\dot{\boldsymbol{q}}_{f_i}} = \tag{24} $$

$$ \begin{bmatrix} -{}^v\boldsymbol{\eta}_i^T \int_0^{l_i} {}^v\boldsymbol{\phi}_i'{}^v\boldsymbol{\phi}_i'^T dx & -{}^w\boldsymbol{\eta}_i^T \int_0^{l_i} {}^w\boldsymbol{\phi}_i'{}^w\boldsymbol{\phi}_i'^T dx & 0 \\ {}^v\boldsymbol{\phi}_{l_i}^T & -{}^\alpha\boldsymbol{\eta}_i^T \int_0^{l_i}\int_0^x {}^\alpha\boldsymbol{\phi}_i{}^w\boldsymbol{\phi}_i''^T d\xi dx & -{}^w\boldsymbol{\eta}_i^T \int_0^{l_i}\int_0^x {}^w\boldsymbol{\phi}_i''{}^\alpha\boldsymbol{\phi}_i^T d\xi dx \\ {}^\alpha\boldsymbol{\eta}_i^T \int_0^{l_i}\int_0^x {}^\alpha\boldsymbol{\phi}_i{}^v\boldsymbol{\phi}_i''^T d\xi dx & {}^w\boldsymbol{\phi}_{l_i}^T & {}^v\boldsymbol{\eta}_i^T \int_0^{l_i}\int_0^x {}^v\boldsymbol{\phi}_i''{}^\alpha\boldsymbol{\phi}_i^T d\xi dx \end{bmatrix} $$

Since the local Jacobian matrices are dependent upon the flexible generalized coordinates' vector, a numerical implementation of (23) and (24) is not pratical. In Appendix C, the space and time dependent terms are separated, enabling an offline computation of these matrices.

We transform the local Jacobian matrices of translation $\boldsymbol{J}_{T,i/i-1}$ and rotation $\boldsymbol{J}_{R,i/i-1}$ from $\mathcal{R}_{i-1}$ to the inertial frame $\mathcal{R}_0$ using the following equation:

$$\begin{aligned} \boldsymbol{J}_{T,i/i-1} &= \boldsymbol{R}_{i-1}^{0}\ {}^{i-1}\boldsymbol{J}_{T,i/i-1} \\ \boldsymbol{J}_{R,i/i-1} &= \boldsymbol{R}_{i-1}^{0}\ {}^{i-1}\boldsymbol{J}_{R,i/i-1} \end{aligned} \tag{25}$$

Jacobian sub-matrix for a flexible link Replacing $\dot{\boldsymbol{r}}_{i/i-1} = \boldsymbol{J}_{T,i/i-1}\dot{\boldsymbol{q}}_{f_i}$ and $\boldsymbol{\omega}_{i/i-1} = \boldsymbol{J}_{R,i/i-1}\dot{\boldsymbol{q}}_{f_i}$ in (5) and (6), and eliminating the generalized velocities yields the following expression for the endpoint Jacobian sub-matrix of a flexible link:

$$(\boldsymbol{J}_e)_{f_i} = \begin{bmatrix} (\boldsymbol{J}_{T,e})_{f_i} \\ (\boldsymbol{J}_{R,e})_{f_i} \end{bmatrix} = \begin{bmatrix} \boldsymbol{J}_{T,i/i-1} - \boldsymbol{r}_{e/i} \times \boldsymbol{J}_{R,i/i-1} \\ \boldsymbol{J}_{R,i/i-1} \end{bmatrix} \in \Re^{6,n_{f_i}} \tag{26}$$

Both the Jacobian column for a joint (3) and the Jacobian sub-matrix for a flexible link (26) have a similar form. Computation of the Jacobian sub-matrix for a flexible link is done in one step once the local Jacobian matrices have been computed.

The position vector $\boldsymbol{r}_{e/i}$ and the rotation matrix $\boldsymbol{R}_i^0$ can be computed recursively as follows:

$$\boldsymbol{R}_i^0 = \boldsymbol{R}_{i-1}^0 \boldsymbol{R}_i^{i-1} \tag{27}$$

$$\boldsymbol{r}_{e/i} = \boldsymbol{r}_{e/i+1} + \boldsymbol{r}_{i+1/i} \tag{28}$$

For a flexible link, the rotation matrix is given by (16) and the position vector by (18). When the frame fixed at the root of the flexible link, $\mathcal{S}_{i-1}$ does not coincide with the joint frame $\mathcal{R}_{i-1}$, a constant rotation and a constant translation must be added.

2.4 Conclusions of the Theoretical Part

The column of the Jacobian corresponding to a joint and the sub-matrix of the Jacobian corresponding to a flexible link were obtained in a compact form using the robot parameters. For a *joint*, only the joint axis and the position vector between the joint and the robot endpoint are needed. For a *flexible link*, both the position vector between the link extremity and the robot endpoint, and the local Jacobian matrices of translation and rotation are required. The method developed is completely general for robots with flexible links characterized by the Euler-Bernoulli model plus a torsional deformation.

Apart from obtaining the endpoint velocities as described by (1) the endpoint Jacobian is useful in determining the generalized force vector $\boldsymbol{Q}$ due to endpoint force and torque $\boldsymbol{f}_e$ as given by the following relation:

$$\boldsymbol{Q} = \boldsymbol{J}_e^T \boldsymbol{f}_e \tag{29}$$

where $\boldsymbol{f}_e = \begin{bmatrix} f_x & f_y & f_z & m_x & m_y & m_z \end{bmatrix}^T$. The generalized force vector has the same meaning as in Lagrange's equations. For a revolute motor with the angle of rotation taken as a generalized coordinate, the generalized force corresponds to the motor torque.

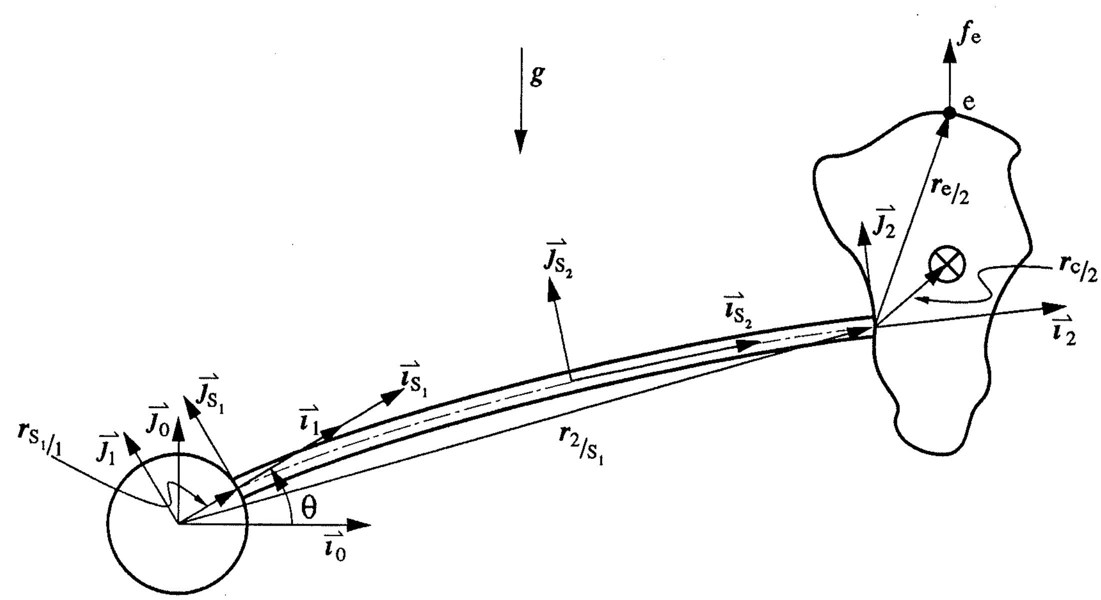

Figure 4: One-link flexible robot

3 Example

We will now illustrate the development of the endpoint Jacobian using an example with a one-link flexible robot. The theoretical results generated by this example will be verified experimentally in Section 4.

3.1 The Kinematics

The one-link flexible robot used in this example is shown in Figure 4. The robot consists of a single flexible link rotating in a vertical plane. The base of the link is clamped in a hub rotating in the (x_0, y_0) plane around the z_0 axis. A tool with an eccentric mass center is attached to the end. This example is similar to the one given by Kozel et al. (1991) , the main difference being that our link rotates in a vertical plane implying that gravity must be taken into account. Because the motion is planar, only the bending within the plane $v(x,t)$ is retained.

First, we calculate the rotation matrices. From Figure 4, we see that the motor rotates around the $\vec{\boldsymbol{k}}_0$ axis which gives the following rotation matrix:

$$\boldsymbol{R}_1^0 = \begin{bmatrix} \cos\theta & -\sin\theta & 0 \\ \sin\theta & \cos\theta & 0 \\ 0 & 0 & 1 \end{bmatrix} \tag{30}$$

Since $\mathcal{R}_1$ and $\mathcal{S}_1$ are parallel, the rotation matrix between these two frames is the identity matrix $\boldsymbol{E}$. Using the rotation matrix for a flexible link (16), the rotation matrix between

$\mathcal{S}_2$ and $\mathcal{R}_1$ is written as:

$$\boldsymbol{R}^1_{\mathcal{S}_2} = \begin{bmatrix} 1-\frac{1}{2}v'^2 & -v' & 0 \\ v' & 1-\frac{1}{2}v'^2 & 0 \\ 0 & 0 & 1 \end{bmatrix} \tag{31}$$

The rotation matrix between $\mathcal{R}_2$ and $\mathcal{R}_1$ is deduced from $\boldsymbol{R}^1_{\mathcal{S}_2}$ by setting $x = l$ in (31).

The different position vectors are now needed. We define the position vector of the tool extremity e with respect to the link extremity (Fig. 4) as:

$$^2\boldsymbol{r}_{e/2} = l_{2_x}\vec{\imath}_2 + l_{2_y}\vec{\jmath}_2 \quad \text{and} \quad \boldsymbol{r}_{e/2} = \boldsymbol{R}^0_2\,{}^2\boldsymbol{r}_{e/2} \tag{32}$$

The tool extremity with respect to the motor axis is then:

$$\boldsymbol{r}_{e/1} = \boldsymbol{r}_{e/2} + \boldsymbol{R}^0_1({}^1\boldsymbol{r}_{2/\mathcal{S}_1} + {}^1\boldsymbol{r}_{\mathcal{S}_1/1}) \tag{33}$$

where:

$$^1\boldsymbol{r}_{\mathcal{S}_1/1} = l_{1_x}\vec{\imath}_1$$

The position of the link extremity with respect to its base is deduced from the position vector for a flexible link (18) by taking $x = l$, which gives the following result:

$$^1\boldsymbol{r}_{2/\mathcal{S}_1} = \begin{bmatrix} l - \frac{1}{2}\int_0^x v'^2\, d\xi \\ v_l \\ 0 \end{bmatrix}$$

where $v_l = v(l,t)$.

3.2 Discretization

The assumed-mode method is used to discretize the continuous coordinate $v(x,t)$ as follows:

$$v(x,t) = \boldsymbol{\phi}^T\boldsymbol{\eta} \tag{34}$$

Then the vector of generalized coordinates for the system is composed of the motor rotation and of the time dependent part of the deformation:

$$\boldsymbol{q} = \begin{bmatrix} \theta \\ \boldsymbol{\eta} \end{bmatrix} \tag{35}$$

3.3 The Jacobian

The Jacobian can now be computed. For the motor, we apply the Jacobian column for a joint (3) to obtain:

$$(\boldsymbol{J}_e)_{j_1} = \begin{bmatrix} \boldsymbol{a}_1 \times \boldsymbol{r}_{e/1} \\ \boldsymbol{a}_1 \end{bmatrix} \quad \text{with} \quad \boldsymbol{a}_1 = {}^1\boldsymbol{a}_1 = \begin{bmatrix} 0 \\ 0 \\ 1 \end{bmatrix} \tag{36}$$

For the flexible link, we use the Jacobian sub-matrix for a flexible link (26):

$$(\boldsymbol{J}_e)_{f_2} = \begin{bmatrix} \boldsymbol{J}_{T,2/1} - \boldsymbol{r}_{e/2} \times \boldsymbol{J}_{R,2/1} \\ \boldsymbol{J}_{R,2/1} \end{bmatrix} \tag{37}$$

where:

$$^1\boldsymbol{J}_{T,2/1} = \begin{bmatrix} -\boldsymbol{\eta} \int_0^l \boldsymbol{\phi}' \boldsymbol{\phi}'^T dx \\ \boldsymbol{\phi}_l^T \\ 0 \end{bmatrix} \quad \text{and} \quad \boldsymbol{J}_{T,2/1} = \boldsymbol{R}_1^{01}\boldsymbol{J}_{T,2/1}$$

$$^1\boldsymbol{J}_{R,2/1} = \begin{bmatrix} 0 \\ 0 \\ \boldsymbol{\phi}_l'^T \end{bmatrix} \quad \text{and} \quad \boldsymbol{J}_{R,2/1} = \boldsymbol{R}_1^{01}\boldsymbol{J}_{R,2/1}$$

The application of (36) and (37), while neglecting terms of order higher than one, results in the endpoint Jacobian expressed in $\mathcal{R}_0$. However, to have a more compact form, we write the Jacobian in $\mathcal{R}_1$ as follows:

$$^1\boldsymbol{J}_e = \begin{bmatrix} -l_{2_y} - (l_{2_x}\boldsymbol{\phi}_l'^T + \boldsymbol{\phi}_l)\boldsymbol{\eta} & -l_{2_y}\boldsymbol{\phi}_l'^T + \left(l_{2_x}\boldsymbol{\phi}_l'^T\boldsymbol{\phi}_l' + \underline{\int_0^l \boldsymbol{\phi}'^T\boldsymbol{\phi}' dx}\right)\boldsymbol{\eta}^T \\ l_{1_x} + l + l_{2_x} - l_{2_y}\boldsymbol{\phi}_l'^T\boldsymbol{\eta} & \boldsymbol{\phi}_l^T + l_{2_x}\boldsymbol{\phi}_l'^T - l_{2_y}\boldsymbol{\phi}_l'^T\boldsymbol{\phi}_l'\boldsymbol{\eta}^T \\ 0 & 0 \\ 0 & 0 \\ 0 & 0 \\ 1 & \boldsymbol{\phi}_l'^T \end{bmatrix} \tag{38}$$

and:

$$\boldsymbol{J}_e = \boldsymbol{R}_1^{01}\boldsymbol{J}_e$$

The underlined term in (38) is a term which will be missing if only the first order terms are kept in the kinematics.

3.4 Model of the Static Deformation

To simulate the system and compare it with experimental results, we need a model of the deformation. That model will estimate the torque required by the motor to obtain a desired endpoint force and predict the shape of deformation of the beam. We obtain this model using Jourdain's principle (Jourdain 1909) which is often refered to as Kane's method (Piedbœuf 1993). For our static case, Jourdain's principle is essentially the same as d'Alembert's principle. The equation for the force equilibrium given an endpoint force $\boldsymbol{f}_e$ is obtained using the Jacobian (29), and results in the following:

$$\boldsymbol{f} = \boldsymbol{J}_{T,e}^T \boldsymbol{f}_e \tag{39}$$

The vector $\boldsymbol{f}$ corresponds to the equation of force equilibrium without an endpoint force and is obtained using the following equation:

$$\boldsymbol{f} = -\boldsymbol{J}_{R,m}^T \boldsymbol{M}_m - \int_0^l \boldsymbol{J}_{T,dm}^T(\rho \boldsymbol{g})dx - \boldsymbol{J}_{T,c}^T(m_t \boldsymbol{g}) + \left(\frac{\partial V_f}{\partial \boldsymbol{q}}\right)^T \tag{40}$$

where:

$\boldsymbol{M}_m = T_m \vec{\boldsymbol{k}}_1$ is the torque applied by the motor;

$\boldsymbol{g} = -g\vec{\boldsymbol{\jmath}}_0$ is the gravity vector;

$V_f = \int_0^l EI_z v''^2 dx$ is the elastic potential energy of the flexible link with EI_z the rigidity;

ρ is the linear density of the link;

m_t is the mass of the tool.

The Jacobian matrices required in (40) can be computed using the general equations for the Jacobian developed previously (eqs (3) and (26)). To reach this goal, we use the fact that the motion of body i depends only on the motion of the bodies 1 to $i-1$ and is not affected by the bodies coming after in the chain (this is true only for an open loop chain). In other words, if we want the Jacobian at a given point, we employ that point as the robot extremity. Hence, we define the three Jacobian matrices required in (40) as follows:

$\boldsymbol{J}_{R,m}$ is the Jacobian of rotation defined by setting the motor as the endpoint, then $e \rightarrow 1$;

$\boldsymbol{J}_{T,dm}$ is the Jacobian of translation defined by setting the position of an element dm (it is equal to the position of $\mathcal{S}_2$) as the endpoint, then $e \rightarrow \mathcal{S}_2$;

$\boldsymbol{J}_{T,c}$ is the Jacobian of translation defined by setting the position of the center of mass of the tool as the endpoint, then $e \rightarrow c$. The position of the center of mass of the tool is: ${}^2\boldsymbol{r}_{c/2} = l_{c_x}\vec{\boldsymbol{\imath}}_2 + l_{c_y}\vec{\boldsymbol{\jmath}}_2$.

After some manipulations made using the symbolic computation software MAPLE, we obtain the equations (41) and (42) for the force equilibrium. To simplify, we split $\boldsymbol{f}$ in two; f_m is a scalar corresponding to the motor and $\boldsymbol{f}_l$ is a vector corresponding to the flexible link. To be consistent with assumption A5, we only retain terms of zero and first order. For f_m, we have:

$$\begin{aligned} f_m &= -T_m + \rho g C l_{1_x} l + \frac{1}{2}\rho g C l^2 - m_t g\left(S l_{c_y} + C(l_{1_x} + l + l_{c_x})\right) \\ &\quad - \left[m_t g(C l_{c_y}\boldsymbol{\phi}_l'^T - S l_{c_x}\boldsymbol{\phi}_l'^T - m_t g S \boldsymbol{\phi}_l^T - \rho g S \int_0^l \boldsymbol{\phi}^T dx\right]\boldsymbol{\eta} \end{aligned} \tag{41}$$

where $S = \sin\theta$ and $C = \cos\theta$. For $\boldsymbol{f}_l$, we have:

$$\begin{aligned} \boldsymbol{f}_l &= \rho g C \int_0^l \boldsymbol{\phi} dx + m_t g\left(C l_{c_x}\boldsymbol{\phi}_l' - S l_{c_y}\boldsymbol{\phi}_l' + C\boldsymbol{\phi}_l\right) + \Bigg[\underline{-\rho g S \int_0^l \int_0^x \boldsymbol{\phi}'\boldsymbol{\phi}'^T d\xi dx} \\ &\quad - m_t g\left(C l_{c_y}\boldsymbol{\phi}_l'\boldsymbol{\phi}_l'^T + S l_{c_x}\boldsymbol{\phi}_l'\boldsymbol{\phi}_l'^T + \underline{S\int_0^l \boldsymbol{\phi}'\boldsymbol{\phi}'^T dx}\right) + EI_z \int_0^l \boldsymbol{\phi}''\boldsymbol{\phi}''^T dx\Bigg]\boldsymbol{\eta} \end{aligned} \tag{42}$$

The underlined terms in (42) affect the stiffness and will be missing if only the first order kinematics is used. They are related to the gravity forces, which means that a beam rotating in a horizontal plane will not have these terms.

For a given endpoint force $\boldsymbol{f}_e$ applied for a known motor angle, the unknowns in (39) are the motor torque T_m and the n_f generalized coordinates associated with the flexible link. Since the vectorial equation (39) gives $1 + n_f$ scalar equations and since these equations are linear in T_m and $\boldsymbol{\eta}$, the solution is easily found.

3.5 Shape functions

To compute the vector $\boldsymbol{f}$ and the endpoint Jacobian $\boldsymbol{J}_e$, we need to select a set of shape functions. When dealing with static deformations, it is known that for linear strain-displacement relationships, the shape of the beam is described by a polynomial of fourth order (Gere and Timoshenko 1990). In our case, the shape function is the solution of the following differential equation:

$$EI_z \frac{d^4 v(x)}{dx} + \rho g \cos\theta = 0 \tag{43}$$

with four boundary conditions reflecting the embedding in the base and the force and torque at the endpoint. However, by including the second order terms in the kinematics, the solution becomes more complex and a fourth order polynomial is not sufficient (see e.g. Gere and Timoshenko 1990, sect. 7.12). Therefore, five shape functions are used each consisting of a simple polynomial of the form:

$$\phi_i(x) = x^{i+1} \text{ with } i = 1, \cdots, 5 \tag{44}$$

The first polynomial is x^2 because the boundary conditions at $x = 0$ imply that $\phi_i(0) = \phi_i'(0) = 0$. To verify, we compare the results for the first order kinematics using three assumed modes with the exact solution obtained by solving the differential equation (43) with its boundary conditions. The two models agree perfectly. After ensuring that the contribution of the higher modes is small, we choose to stop at five modes for the second order kinematics.

4 Experimental Apparatus

The experimental apparatus used to validate the model developed in the example is shown in figure 5. It consists of a small DC motor onto which a torque sensor is mounted. The flexible arm is fixed on the torque sensor, and at the end of the flexible arm is the tool. The force is applied at the end of the tool using different masses. The parameters of the experimental apparatus are displayed in Table 1. Since the flexible arm rotates in the vertical plane, the endpoint force is always along the $\vec{\jmath}_0$ axis and the components along $\vec{\imath}_0$ and $\vec{k}_0$ are zero.

4.1 Experimental Procedures

We validate the model developed in the previous section by varying the endpoint force f_{e_y} from 0 to -6 N and the motor angle θ_m from -90^o to 90^o by 30^o increments (except for the last force where 15^o increments are used from 0^o to 90^o). The vector of the experimental values for the endpoint force is shown in Table 1. We use a PID controller to maintain the motor at a desired angle, and for each angle we measure the motor torque as given by the torque sensor and the beam curvatures using the three strain gauges. We calibrate the strain gauges using the 0^o position (Fig.4) with zero endpoint force. We then take all the curvature measurements with respect to the calibration position.

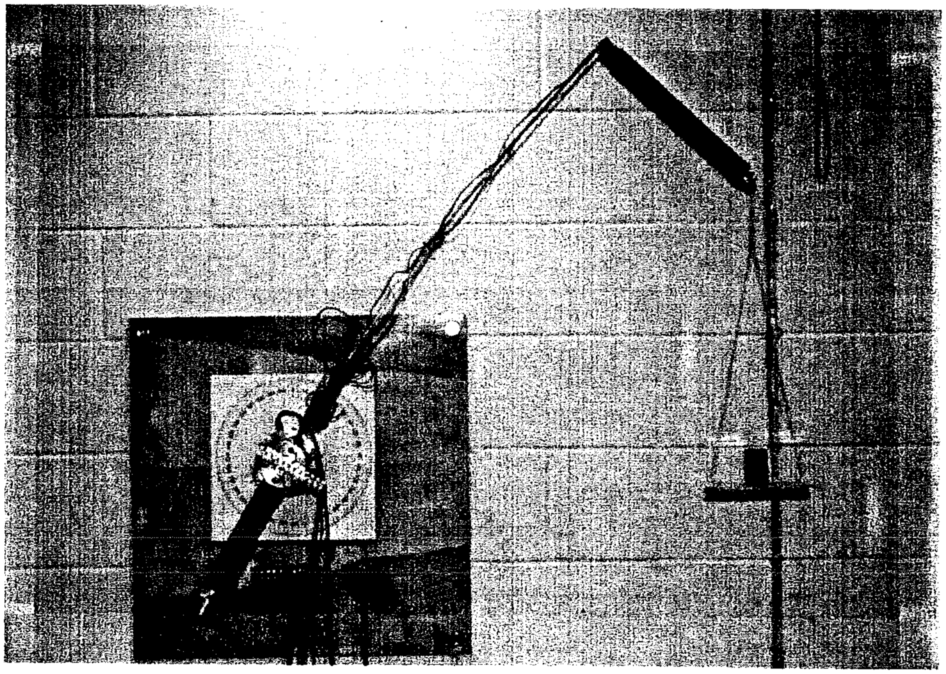

Figure 5: Experimental setup

Hub:	*radius*	$l_{1_x} = 0.0365\ m$
Link:	*length*	$l = 0.7845\ m$
	stiffness	$EI_z = 13.4\ Nm^2$
	linear density	$\rho = 0.650\ kg/m$
Tool:	*mass*	$m_t = 0.1608\ kg$
	endpoint	$l_{2_x} = 0.0115\ m$
		$l_{2_y} = -0.3159\ m$
	mass center	$l_{c_x} = 0.0115\ m$
		$l_{c_y} = -0.158\ m$
Strain gauges:	*position*	$x_{g_1} = 0.0191\ m$
		$x_{g_2} = 0.3985\ m$
		$x_{g_3} = 0.5889\ m$
Endpoint force:		
$f_{e_y} = \begin{bmatrix} 0 & -0.61 & -1.22 & -1.84 & -2.46 & -4.19 & -5.4 \end{bmatrix} N$		

Table 1: Parameters of the experimental apparatus

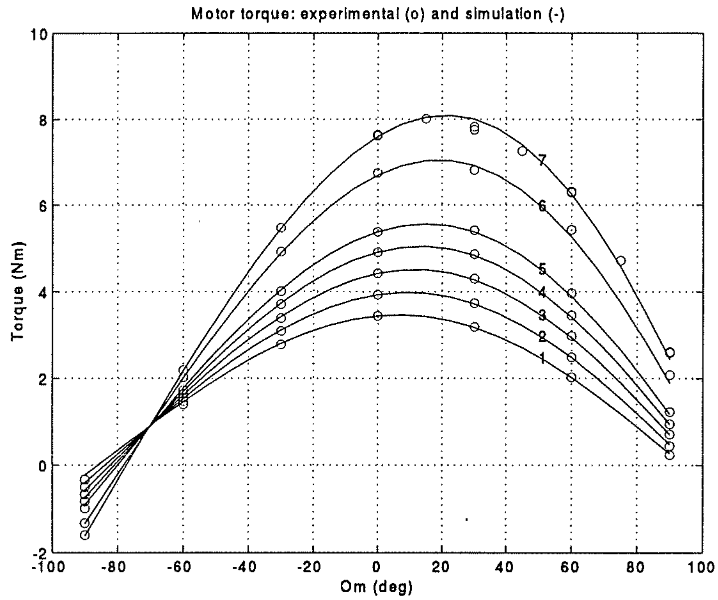

Figure 6: Torque required by the motor in function of f_{e_y} and θ_m using Model $\mathcal{O}(2)$ and comparison with experimental values

4.2 Simulation and Experimental Results

In this section, we demonstrate that our model, using second order kinematics is closer to the experimental results than models neglecting it. We also show the differences between the models. To simplify, we use $\mathcal{O}(2)$ for the model including the second order terms in the kinematics, $\mathcal{O}(1)$ for the model excluding it, and $\mathcal{O}(0)$ for the model neglecting the flexibility of the link (assuming a rigid link). On each of the graphs, the curves are numbered from 1 to 7 corresponding to the seven different endpoint forces defined in Table 1: curve number i correponds to $\boldsymbol{f}_{e_y}[i]$. As we will see later, the last two endpoint forces result in endpoint deformations that are outside of the 10% limit defined in assumption A5. We still keep them to see how well the models behave outside the limit.

The graph in Figure 6 shows the torque required by the motor as predicted by the model including the second order terms. It also shows the experimental results measured using the torque sensor. Model $\mathcal{O}(2)$ closely approximates the experimental results even for the curves 6 and 7 which are outside the 10% limit. The next two graphs, in Figure 7 and Figure 8, concern the motor torque and illustrate the difference between the second order kinematics model and the first and zero order kinematics models. There is no significant difference between the models $\mathcal{O}(2)$ and $\mathcal{O}(1)$: less than 1% for Curve 5 and less than 2% for Curve 7 (which is outside the models limit). However, if the rigid model ($\mathcal{O}(0)$) is used, the error is greater than 8% for Curve 5 and 12% for Curve 7.

The graph of Figure 9 shows the curvature of the first strain gauge as obtained from the simulation of Model $\mathcal{O}(2)$ compared with the experimental curvatures. In Figure 10, we compare the same experimental curvatures to Model $\mathcal{O}(1)$. Model $\mathcal{O}(2)$ closely approximates the experimental curvatures even for forces 6 and 7. This is certainly not the case for Model $\mathcal{O}(1)$ which shows significant differences even for forces resulting in deformations

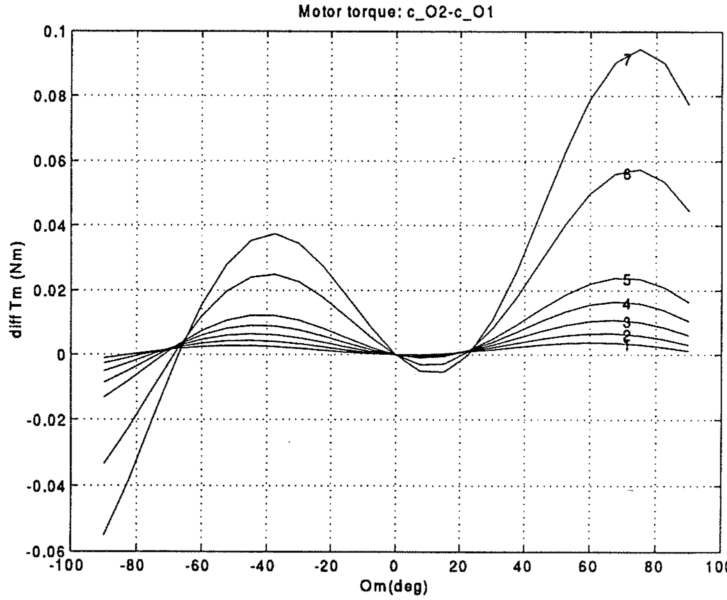

Figure 7: Torque required by the motor in function of f_{e_y} and θ_m: difference between models $\mathcal{O}(2)$ and $\mathcal{O}(1)$

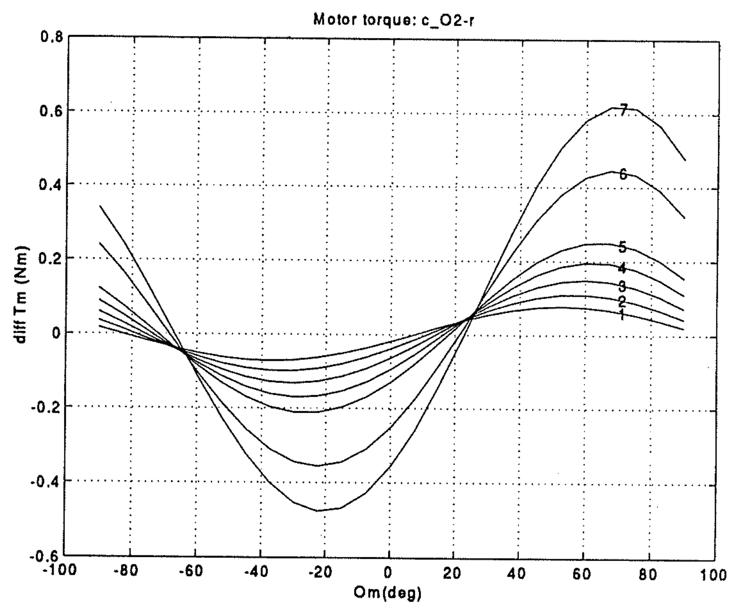

Figure 8: Torque required by the motor in function of f_{e_y} and θ_m: difference between models $\mathcal{O}(2)$ and $\mathcal{O}(0)$

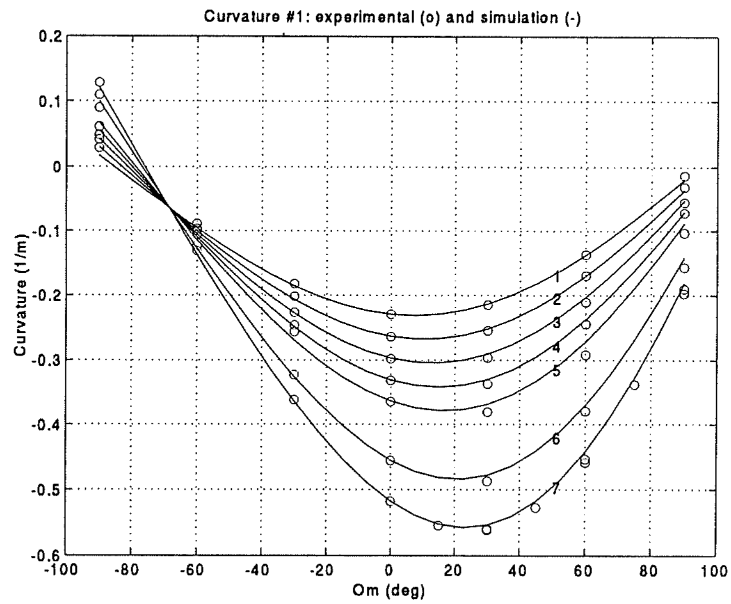

Figure 9: Curvature of the first strain gauge in function of f_{e_y} and θ_m for Model $\mathcal{O}(2)$ and comparison with experimental values

inside the model limit.

Figure 11 shows the simulated endpoint deformation for Model $\mathcal{O}(2)$. The maximum deflection in Figure 11 is almost -12 *cm* at 45^o. As aforementioned, with a link length of approximatively 0.8 *m*, -12 *cm* is more than 1.5 times the maximum permissible deformation while working under the 10% limit of assumption A5. Still, as noted previously, torque and curvatures predicted by Model $\mathcal{O}(2)$ well agree with the experimental results for all the endpoint forces. Figure 12 illustrates the difference between the endpoint deformation predicted by models $\mathcal{O}(2)$ and $\mathcal{O}(1)$. This difference is more than 5 *mm* for Curve 5 and more than 13 *mm* for Curve 7. Such a difference is important for robotic applications where a precision of less than one millimeter is not unusual.

From the comparison of the different models with the experimental results, we reach the following conclusions:

1) There is no major difference between the torque predicted by the models using first and second order kinematics. However significant errors result when the rigid model is employed.

2) The curvature is well predicted by the second order kinematics model but large errors occur when only first order kinematics is used.

3) The difference between the endpoint position as predicted by the second order kinematics and the first order kinematics models, is significant enough to conclude that the model using only the first order kinematics is misleading.

4) The second order kinematics model well predict the experimental results even outside the 10% deformation limit.

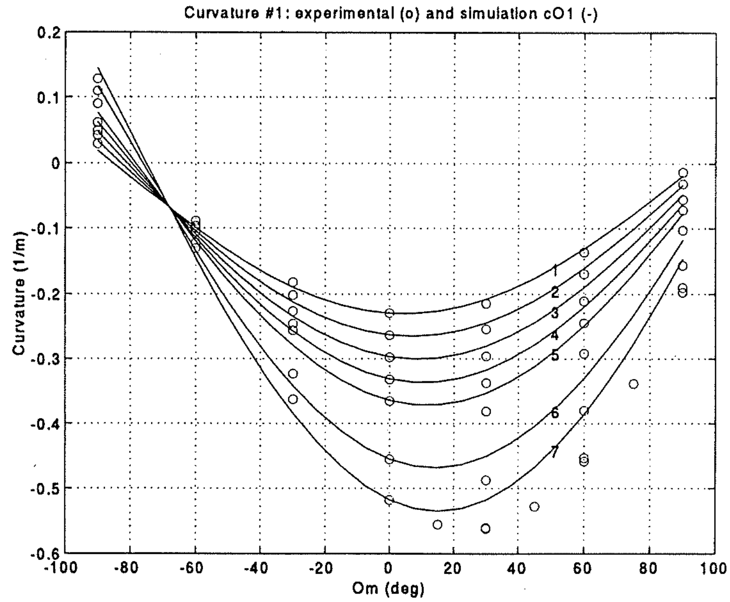

Figure 10: Curvature of the first strain gauge in function of f_{e_y} and θ_m for Model $\mathcal{O}(1)$ and comparison with experimental values

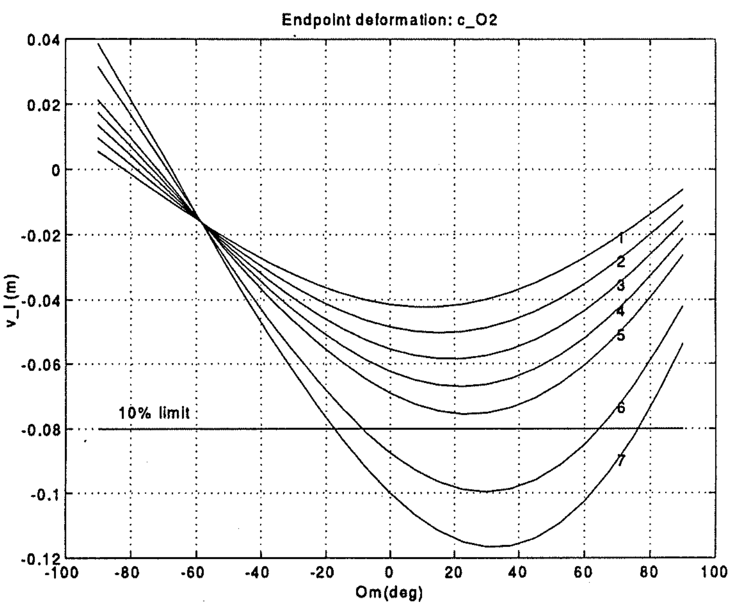

Figure 11: Endpoint deformation in function of f_{e_y} and θ_m for Model $\mathcal{O}(2)$

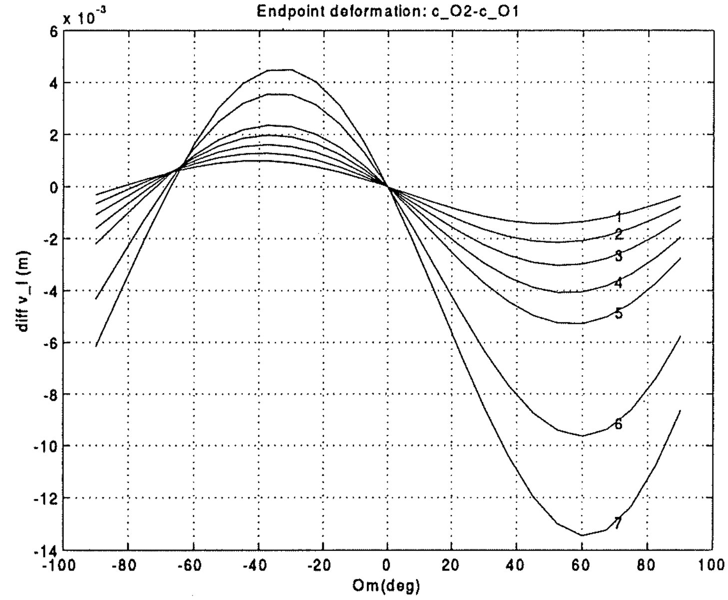

Figure 12: Endpoint deformation in function of f_{e_y} and θ_m: difference between models $\mathcal{O}(2)$ and $\mathcal{O}(1)$

As a general remark, we think that discussing the geometric stiffening effect only in terms of angular speed is insufficient with the exception, perhaps, of the cases of one-link flexible beams rotating in the horizontal plane without endpoint force. The term *stiffening effect* is in itself misleading since some of the effects resulting from the inclusion of the second order kinematics, are softening ones.

5 Conclusion

In this paper, we developed the endpoint Jacobian exact to the first order for a general tree-like manipulator with flexible links, using second order kinematics. Similarly to rigid robot methods, we wrote the Jacobian in terms of the joint axis, the link deformations and the relative position vectors using cross products. A column of the Jacobian matrix correspondes to each joint, and a sub-matrix to each flexible link. To override the problem of choosing an order of rotation for the section of a flexible link, we chose the curvatures and the twist as generalized coordinates. Then, we defined two local Jacobian matrices relating the extremity of a flexible link to its root. Using these matrices, we determined the endpoint Jacobian sub-matrix using the same formulation as we used for a joint. With an example and experimental results, we conclude that our Jacobian matrix is valid. And finally, in order to closely match experimental results, we have shown that models must include the second order kinematics.

References

[1] H. Asada and J.-J. E. Slotine. *Robot Analysis and Control.* John Wiley and Sons,

1986.

[2] H. Bremer. Dynamik von Mehrkörpersystemen mit elastichen Bauteilen. *ZAMM Z. angew. Math, Mech*, 65(12):613–621, 1985.

[3] H. Bremer. On the dynamics of flexible manipulators. In *1987 IEEE International Conference on Robotics and Automation*, pages 1556–1560, 1987.

[4] Harmut Bremer. *Kinetik starr-elasticher Mehrkörpersysteme.* Fortschrittberichte der VDI-Z, 983. Reihe 11, Nr. 53.

[5] Hartmut Bremer and Friedrich Pfeiffer. *Elastiche Mehrkörpersystem.* B. G. Teubner Stuttgart, 1992.

[6] Liang-Wey Chang and J.F. Hamilton. The kinematics of robotic manipulators with flexible links using an equivalent rigid link system (ERLS) model. *Transactions of the ASME Journal of Dynamic Systems, Measurement, and Control*, 113:48–53, March 1991.

[7] B. C. Chiou and M. Shahinpoor. Stability considerations for a two-link force-controlled flexible manipulator. In *1990 IEEE International Conference on Robotics and Automation*, pages 728–733, 1990.

[8] James M. Gere and Stephen P. Timoshenko. *Mechanics of materials.* PWS-Kent, 3rd edition, 1990.

[9] Dewey H. Hodges, Robert A. Ormiston, and David A. Peters. *On the Nonlinear Deformation Geometry of Euler-Bernoulli Beams.* Technical Report, NASA, 1980. TP 1566.

[10] S. K. Ider and F. M. L. Amirouche. Nonlinear modeling of flexible multibody systems dynamics subjected to variable constraints. *Transactions of the ASME Journal of Dynamic Systems, Measurement, and Control*, 56:444–450, June 1989.

[11] R. Johanni. *Automatisches Aufstellen der Bewegungsgleichungen von baumstrukturierten Mehrkörpersystemen mit elastischen Bauteilen.* Technical Report 8501, Institute B for Mechanics, Technical University of Munich, 1985.

[12] R. Johanni. On the automatic generation of the equations of motion for robots with elastically deformable arms. In *IFAC/IFIP/IMACS International Symposium on Theory of Robots*, pages 195–199, December 1986.

[13] Philip E. B. Jourdain. Note on an analogue of Gauss' principle of least constraint. *The Quarterly Journal of Pure and Applied Mathematics*, XL:153–157, 1909.

[14] K. R. V. Kaza and R. G. Kvaternik. Nonlinear flag-lag-axial equations of a rotating beam. *AIAA Journal*, 15(6):871–874, June 1977.

[15] D. Kozel, A. J. Koivo, and S. S. Mahil. A general force/torque relationship and kinematic representation for flexible link manipulators. *Journal of Robotic Systems*, 8(4):531–556, 1991.

[16] Junghsen Lieh. An alternative method for formulating closed-form dynamics for elastic mechanical systems using symbolic process. *Mechanism of Structures and Machines*, 20(2):253–279, 1992.

[17] Leonard Meirovitch. *Analytical Methods in Vibrations.* The Macmillan Company, New York, 1967.

[18] Leonard Meirovitch. *Methods of Analytical Dynamics.* McGraw-Hill, New York, 1970.

[19] D. E. Orin and W. W. Schrader. Efficient computation of the Jacobian for robot manipulators. *The International Journal of Robotics Research*, 3(4):66–75, 1984.

[20] Carlos E. Padilla and Andreas H. von Flowtow. Nonlinear strain-displacement relations and flexible multibody dynamics. *Journal of Guidance, Control, and Dynamics*, 15(1):128–136, January 1992.

[21] F. Pfeiffer and H. Bremer. Elastic multibody theory applied to elastic manipulators. In *IUTAM Symposium on: Dynamical Problems of Rigid-Elastic Systems and Structures*, Moscow, May 1990.

[22] F. Pfeiffer, K. Richter, and H. Wapenhans. Elastic robot trajectory planning with force control. In *IFIP International Symposium on Theory of Robots*, Rome, Italy, 1990.

[23] Inna Sharf. Geometric stiffening in multibody dynamics formulations. 1993. Department of Mechanical Engineering, University of Victoria, Victoria BC, Canada, V8W 3P6. Personal communication.

[24] J. C. Simo and L. Vu-Quoc. The role of non-linear theories in transient dynamic analysis of flexible structures. *Journal of Sound and Vibration*, 119(3):487–508, 1987.

[25] J.-C. Piedbœuf. Kane's equation or Jourdain's principle. In *36th Midwest Symposium on Circuits and Systems*, August 1993. Invited paper.

[26] Shui-Lin Weng and Donald T. Greenwood. General dynamical equations of motion for elastic body systems. *Journal of Guidance, Control, and Dynamics*, 15(6):1434–1442, November-December 1992.

[27] Daniel W. Williams and David A. Turcic. An inverse kinematic analysis procedure for flexible open-loop mechanisms. *Mechanism and Machine Theory*, 27(6):701–714, 1992.

A Local Curvatures and Rotation Matrix

In this Appendix, we develop the relation between the local curvatures and the rotation matrix. Assume a vector $\boldsymbol{r}$ fixed in a frame $\mathcal{R}_1$ that is rotated by a small angle vector $\Delta\boldsymbol{\theta}$ with respect to frame $\mathcal{R}_0$. Then ${}^{\mathcal{R}_0}\boldsymbol{r}$, the vector expressed in $\mathcal{R}_0$, is written in terms of ${}^{\mathcal{R}_1}\boldsymbol{r}$ as (Meirovitch 1970):

$$
\begin{aligned}
{}^{\mathcal{R}_0}\boldsymbol{r} &= {}^{\mathcal{R}_1}\boldsymbol{r} + {}^{\mathcal{R}_1}\Delta\boldsymbol{r} && (45)\\
&= \boldsymbol{R}^{\mathcal{R}_0}_{\mathcal{R}_1}\,{}^{\mathcal{R}_1}\boldsymbol{r} && (46)
\end{aligned}
$$

$$= \left[\begin{bmatrix} 1 & 0 & 0 \\ 0 & 1 & 0 \\ 0 & 0 & 1 \end{bmatrix} + \begin{bmatrix} 0 & -\Delta\boldsymbol{\theta}_z & \Delta\boldsymbol{\theta}_y \\ \Delta\boldsymbol{\theta}_z & 0 & -\Delta\boldsymbol{\theta}_x \\ -\Delta\boldsymbol{\theta}_y & \Delta\boldsymbol{\theta}_x & 0 \end{bmatrix} \right] {}^{\mathcal{R}_1}\boldsymbol{r} \tag{47}$$

Equations (45) and (47) give ${}^{\mathcal{R}_1}\Delta\boldsymbol{r}$ in terms of the rotation angles. Considering that the small rotation occurs because of a small translation Δx of the reference frame and taking $\Delta x \to 0$, we derive:

$${}^{\mathcal{R}_1}\boldsymbol{r}' = {}^{\mathcal{R}_1}\tilde{\boldsymbol{\kappa}}\,{}^{\mathcal{R}_1}\boldsymbol{r} \tag{48}$$

where ${}^{\mathcal{R}_1}\tilde{\boldsymbol{\kappa}}$ is defined in (10). This relationship is similar to the one between the angular speed and the rotation matrix for a rotating frame.

Consider now:

$${}^{\mathcal{S}_{i-1}}\boldsymbol{r}_{\mathcal{S}_i/\mathcal{S}_{i-1}} = \boldsymbol{R}_{\mathcal{S}_i}^{\mathcal{S}_{i-1}}\,{}^{\mathcal{S}_i}\boldsymbol{r}_{\mathcal{S}_i/\mathcal{S}_{i-1}} \tag{49}$$

Differentiation of (49) with respect to x gives:

$${}^{\mathcal{S}_{i-1}}\boldsymbol{r}'_{\mathcal{S}_i/\mathcal{S}_{i-1}} = \left(\boldsymbol{R}_{\mathcal{S}_i}^{\mathcal{S}_{i-1}}\right)'\,{}^{\mathcal{S}_i}\boldsymbol{r}_{\mathcal{S}_i/\mathcal{S}_{i-1}} + \boldsymbol{R}_{\mathcal{S}_i}^{\mathcal{S}_{i-1}}\,{}^{\mathcal{S}_i}\boldsymbol{r}'_{\mathcal{S}_i/\mathcal{S}_{i-1}} \tag{50}$$

Using (48), the derivative of (49) with respect to x is also expressed as:

$${}^{\mathcal{S}_{i-1}}\boldsymbol{r}'_{\mathcal{S}_i/\mathcal{S}_{i-1}} = {}^{\mathcal{S}_{i-1}}\tilde{\boldsymbol{\kappa}}\,{}^{\mathcal{S}_{i-1}}\boldsymbol{r}_{\mathcal{S}_i/\mathcal{S}_{i-1}} + \left({}^{\mathcal{S}_{i-1}}\boldsymbol{r}_{\mathcal{S}_i/\mathcal{S}_{i-1}}\right)'_r \tag{51}$$

where $\left({}^{\mathcal{S}_{i-1}}\boldsymbol{r}_{\mathcal{S}_i/\mathcal{S}_{i-1}}\right)'_r = \boldsymbol{R}_{\mathcal{S}_i}^{\mathcal{S}_{i-1}}\,{}^{\mathcal{S}_i}\boldsymbol{r}'_{\mathcal{S}_i/\mathcal{S}_{i-1}}$ is the derivative in the frame $\mathcal{S}_i$. Equality of (50) and (51) gives:

$${}^{\mathcal{S}_{i-1}}\tilde{\boldsymbol{\kappa}}\,{}^{\mathcal{S}_{i-1}}\boldsymbol{r}_{\mathcal{S}_i/\mathcal{S}_{i-1}} = \left(\boldsymbol{R}_{\mathcal{S}_i}^{\mathcal{S}_{i-1}}\right)'\,{}^{\mathcal{S}_i}\boldsymbol{r}_{\mathcal{S}_i/\mathcal{S}_{i-1}} \tag{52}$$

From (52), we can write:

$${}^{\mathcal{S}_{i-1}}\tilde{\boldsymbol{\kappa}}\boldsymbol{R}_{\mathcal{S}_i}^{\mathcal{S}_{i-1}}\,{}^{\mathcal{S}_i}\boldsymbol{r}_{\mathcal{S}_i/\mathcal{S}_{i-1}} = \left(\boldsymbol{R}_{\mathcal{S}_i}^{\mathcal{S}_{i-1}}\right)'\,{}^{\mathcal{S}_i}\boldsymbol{r}_{\mathcal{S}_i/\mathcal{S}_{i-1}} \tag{53}$$

Equation (53) gives a relationship between the curvature expressed in frame $\mathcal{S}_{i-1}$ and the rotation matrix:

$${}^{\mathcal{S}_{i-1}}\tilde{\boldsymbol{\kappa}}\boldsymbol{R}_{\mathcal{S}_i}^{\mathcal{S}_{i-1}} = \left(\boldsymbol{R}_{\mathcal{S}_{i-1}}^{\mathcal{S}_i}\right)' \tag{54}$$

To obtain the curvature in frame $\mathcal{S}_i$, we start again from equation (52) and write:

$$\boldsymbol{R}_{\mathcal{S}_i}^{\mathcal{S}_{i-1}}\,{}^{\mathcal{S}_i}\tilde{\boldsymbol{\kappa}}\left(\boldsymbol{R}_{\mathcal{S}_i}^{\mathcal{S}_{i-1}}\right)^T \boldsymbol{R}_{\mathcal{S}_{i-1}}^{\mathcal{S}_i}\,{}^{\mathcal{S}_i}\boldsymbol{r}_{\mathcal{S}_i/\mathcal{S}_{i-1}} = \left(\boldsymbol{R}_{\mathcal{S}_i}^{\mathcal{S}_{i-1}}\right)'\,{}^{\mathcal{S}_i}\boldsymbol{r}_{\mathcal{S}_i/\mathcal{S}_{i-1}} \tag{55}$$

Simplification of (55) yields:

$$\boldsymbol{R}_{\mathcal{S}_i}^{\mathcal{S}_{i-1}}\,{}^{\mathcal{S}_i}\tilde{\boldsymbol{\kappa}} = \left(\boldsymbol{R}_{\mathcal{S}_i}^{\mathcal{S}_{i-1}}\right)' \tag{56}$$

B Rotation Matrix and Position Vector

In this Appendix, we write the rotation matrix and position vector directly in terms of the curvature. The solutions of (13) and (14) in terms of the curvatures are the following:

$$\boldsymbol{R}_1 = \begin{bmatrix} 0 & -\int_0^x \kappa_z d\xi & \int_0^x \kappa_y d\xi \\ \int_0^x \kappa_z d\xi & 0 & -\int_0^x \kappa_x d\xi \\ -\int_0^x \kappa_y d\xi & \int_0^x \kappa_x d\xi & 0 \end{bmatrix} \tag{57}$$

$$\boldsymbol{R}_2 = \begin{bmatrix} -\frac{1}{2}\left(\int_0^x \kappa_z d\xi\right)^2 - \frac{1}{2}\left(\int_0^x \kappa_y d\xi\right)^2 & \int_0^x \left(\int_0^\xi \kappa_y d\eta\right) \kappa_x d\xi & \int_0^x \left(\int_0^\xi \kappa_z d\eta\right) \kappa_x d\xi \\ \int_0^x \left(\int_0^\xi \kappa_x d\eta\right) \kappa_y d\xi & -\frac{1}{2}\left(\int_0^x \kappa_z d\xi\right)^2 - \frac{1}{2}\left(\int_0^x \kappa_x d\xi\right)^2 & \int_0^x \left(\int_0^\xi \kappa_z d\eta\right) \kappa_y d\xi \\ \int_0^x \left(\int_0^\xi \kappa_x d\eta\right) \kappa_z d\xi & \int_0^x \left(\int_0^\xi \kappa_y d\eta\right) \kappa_z d\xi & -\frac{1}{2}\left(\int_0^x \kappa_y d\xi\right)^2 - \frac{1}{2}\left(\int_0^x \kappa_x d\xi\right)^2 \end{bmatrix} \tag{58}$$

The position vector (18) written in terms of the curvatures is expressed as follows:

$$\boldsymbol{r}_{S_{i-1},S_i} = \begin{bmatrix} x - \int_0^x \left\{ \frac{1}{2}\left(\int_0^\xi \kappa_z d\eta\right)^2 + \frac{1}{2}\left(\int_0^\xi \kappa_y d\eta\right)^2 \right\} d\xi \\ \int_0^x \left(\int_0^\xi \kappa_z d\eta\right) d\xi + \int_0^x \left\{ \int_0^\xi \left(\int_0^\eta \kappa_x d\zeta\right) \kappa_y d\eta \right\} d\xi \\ \int_0^x \left(\int_0^\xi -\kappa_y d\eta\right) d\xi + \int_0^x \left\{ \int_0^\xi \left(\int_0^\eta \kappa_x d\zeta\right) \kappa_z d\eta \right\} d\xi \end{bmatrix} \tag{59}$$

C Local Jacobian Matrices

The local Jacobian matrices can be separated into zero and first order components as shown in this Appendix. This renders computer implementation easier. Because we divide the space-dependent from the time-dependent variables, main parts of the local Jacobian matrices can be computed in advance.

$${}^{i-1}\boldsymbol{J}_{R,i/i-1} = \underbrace{({}^{i-1}\boldsymbol{J}_{R,i/i-1})_0}_{0^{th}\ order} + \underbrace{({}^{i-1}\boldsymbol{J}_{R,i/i-1})_1}_{1^{st}\ order} \tag{60}$$

$${}^{i-1}\boldsymbol{J}_{T,i/i-1} = \underbrace{({}^{i-1}\boldsymbol{J}_{T,i/i-1})_0}_{0^{th}\ order} + \underbrace{({}^{i-1}\boldsymbol{J}_{T,i/i-1})_1}_{1^{st}\ order} \tag{61}$$

$$ {}^{i-1}\boldsymbol{J}_{T,i/i-1},\, {}^{i-1}\boldsymbol{J}_{R,i/i-1} \in \Re^{3,n_{f_i}} $$

where $()_0$ refers to a zero order term and $()_1$ to a first order term. The definitions of the local Jacobian matrices of rotation of zero and first order are:

$$ ({}^{i-1}\boldsymbol{J}_{R,i/i-1})_0 \overset{\mathcal{O}(0)}{=} \frac{\partial\, {}^{i-1}\boldsymbol{\omega}_{i/i-1}}{\partial \dot{\boldsymbol{q}}_{f_i}} = \begin{bmatrix} 0 & 0 & {}^{\alpha}\phi_i^T \\ 0 & -{}^{w}\phi_i'^T & 0 \\ {}^{v}\phi_i'^T & & 0 \end{bmatrix} \qquad ({}^{i-1}\boldsymbol{J}_{R,i/i-1})_1 = \begin{bmatrix} \boldsymbol{q}_{f_i}^T \boldsymbol{J}_{Rx,i} \\ \boldsymbol{q}_{f_i}^T \boldsymbol{J}_{Ry,i} \\ \boldsymbol{q}_{f_i}^T \boldsymbol{J}_{Rz,i} \end{bmatrix} \tag{62} $$

with:

$$ \boldsymbol{J}_{Rx,i} = \frac{\partial}{\partial \dot{\boldsymbol{q}}_{f_i}} \left(\frac{\partial ({}^{i-1}\boldsymbol{\omega}_{i/i-1})_x}{\partial \dot{\boldsymbol{q}}_{f_i}} \right) = \begin{bmatrix} 0 & \int_0^{l_i} {}^{v}\phi_i' {}^{w}\phi_i''^T dx & 0 \\ -\int_0^{l_i} {}^{w}\phi_i' {}^{v}\phi_i''^T dx & 0 & 0 \\ 0 & 0 & 0 \end{bmatrix} $$
$$ \boldsymbol{J}_{Ry,i} = \frac{\partial}{\partial \dot{\boldsymbol{q}}_{f_i}} \left(\frac{\partial ({}^{i-1}\boldsymbol{\omega}_{i/i-1})_y}{\partial \dot{\boldsymbol{q}}_{f_i}} \right) = \begin{bmatrix} 0 & 0 & \int_0^{l_i} {}^{v}\phi_i' {}^{\alpha}\phi_i'^T dx \\ 0 & 0 & 0 \\ -\int_0^{l_i} {}^{\alpha}\phi_i' {}^{v}\phi_i''^T dx & 0 & 0 \end{bmatrix} \tag{63} $$
$$ \boldsymbol{J}_{Rz,i} = \frac{\partial}{\partial \dot{\boldsymbol{q}}_{f_i}} \left(\frac{\partial ({}^{i-1}\boldsymbol{\omega}_{i/i-1})_z}{\partial \dot{\boldsymbol{q}}_{f_i}} \right) = \begin{bmatrix} 0 & 0 & 0 \\ 0 & 0 & \int_0^{l_i} {}^{w}\phi_i' {}^{\alpha}\phi_i'^T dx \\ 0 & -\int_0^{l_i} {}^{\alpha}\phi_i' {}^{w}\phi_i'^T dx & 0 \end{bmatrix} $$

where $({}^{i-1}\boldsymbol{\omega}_{i/i-1})_x$ means the x component of ${}^{i-1}\boldsymbol{\omega}_{i/i-1}$ (similarly for y and z). Define in the same manner, the local Jacobian matrices of translation are:

$$ ({}^{i-1}\boldsymbol{J}_{T,i/i-1})_0 \overset{\mathcal{O}(0)}{=} \frac{\partial\, {}^{i-1}\dot{\boldsymbol{r}}_{i/i-1}}{\partial \dot{\boldsymbol{q}}_{f_i}} = \begin{bmatrix} 0 & 0 & 0 \\ {}^{v}\phi_i^T & 0 & 0 \\ 0 & {}^{w}\phi_i^T & 0 \end{bmatrix} \qquad ({}^{i-1}\boldsymbol{J}_{T,i/i-1})_1 = \begin{bmatrix} \boldsymbol{q}_{f_i}^T \boldsymbol{J}_{Tx,i} \\ \boldsymbol{q}_{f_i}^T \boldsymbol{J}_{Ty,i} \\ \boldsymbol{q}_{f_i}^T \boldsymbol{J}_{Tz,i} \end{bmatrix} \tag{64} $$

with:

$$ \boldsymbol{J}_{Tx,i} = \frac{\partial}{\partial \boldsymbol{q}_{f_i}} \left(\frac{\partial ({}^{i-1}\dot{\boldsymbol{r}}_{i/i-1})_x}{\partial \dot{\boldsymbol{q}}_{f_i}} \right) = \begin{bmatrix} -\int_0^{l_i} {}^{v}\phi_i' {}^{v}\phi_i'^T dx & 0 & 0 \\ 0 & -\int_0^{l_i} {}^{w}\phi_i' {}^{w}\phi_i'^T dx & 0 \\ 0 & 0 & 0 \end{bmatrix} $$
$$ \boldsymbol{J}_{Ty,i} = \frac{\partial}{\partial \dot{\boldsymbol{q}}_{f_i}} \left(\frac{\partial (\Delta \boldsymbol{r}_i)_y}{\partial \dot{\boldsymbol{q}}_{f_i}} \right) = \begin{bmatrix} 0 & 0 & 0 \\ 0 & 0 & -\int_0^{l_i}\int_0^{x} {}^{w}\phi_i'' {}^{\alpha}\phi_i^T d\xi dx \\ 0 & -\int_0^{l_i}\int_0^{x} {}^{\alpha}\phi_i {}^{w}\phi_i''^T d\xi dx & 0 \end{bmatrix} \tag{65} $$
$$ \boldsymbol{J}_{Tz,i} = \frac{\partial}{\partial \boldsymbol{q}_{f_i}} \left(\frac{\partial ({}^{i-1}\dot{\boldsymbol{r}}_{i/i-1})_z}{\partial \dot{\boldsymbol{q}}_{f_i}} \right) = \begin{bmatrix} 0 & 0 & \int_0^{l_i}\int_0^{x} {}^{v}\phi_i'' {}^{\alpha}\phi_i^T d\xi dx \\ 0 & 0 & 0 \\ \int_0^{l_i}\int_0^{x} {}^{\alpha}\phi_i {}^{v}\phi_i''^T d\xi dx & 0 & 0 \end{bmatrix} $$

As indicated by (62) and (64), zero-order local Jacobians $(\boldsymbol{J}_{T,i/i-1})_0$ and $(\boldsymbol{J}_{R,i/i-1})_0$ are constant when defined in the $\mathcal{R}_{i-1}$ frame. This is not true for first-order local Jacobians $(\boldsymbol{J}_{T,i/i-1})_1$ and $(\boldsymbol{J}_{R,i/i-1})_1$, which depend upon the flexible coordinates vector $\boldsymbol{q}_{f_i}$, which is defined as follows:

$$ \boldsymbol{q}_{f_i} = \begin{bmatrix} {}^{v}\eta_i \\ {}^{w}\eta_i \\ {}^{\alpha}\eta_i \end{bmatrix} \tag{66} $$